Title

Temporal and spatial characteristics of the urban heat island in Beijing and the impact on building design and energy performance

Authors

Cui, Ying
Yan, Da
Hong, Tianzhen
et al.

Publication Date

2017-07-01

DOI

10.1016/j.energy.2017.04.053

Peer reviewed

Temporal and spatial characteristics of the urban heat island in Beijing and the impact on building design and energy performance

Ying Cui[a], Da Yan[a,*], Tianzhen Hong[b], Jingjin Ma[c]

[a] School of Architecture, Tsinghua University, Beijing, China

[b] Building Technology and Urban Systems Division, Lawrence Berkeley National Laboratory, Berkeley, California 94720, USA

[c] Beijing Meteorology Service, Beijing, China

* Corresponding author.

E-mail address: yanda@tsinghua.edu.cn (D. Yan).

Abstract

With the increased urbanization in most countries worldwide, the urban heat island (UHI) effect, referring to the phenomenon that an urban area has higher ambient temperature than the surrounding rural area, has gained much attention in recent years. Given that Beijing is developing rapidly both in urban population and economically, the UHI effect can be significant. A long-term measured weather dataset from 1961 to 2014 for ten rural stations and seven urban stations in Beijing, was analyzed in this study, to understand the detailed temporal and spatial characteristics of the UHI in Beijing. The UHI effect in Beijing is significant, with an urban-to-rural temperature difference of up to 8℃ during the winter nighttime. Furthermore, the impacts of UHIs on building design and energy performance were also investigated. The UHI in Beijing led to an approximately 11% increase in cooling load and 16% decrease in heating load in the urban area compared with the rural area, whereas the urban heating peak load decreased 9% and the cooling peak load increased 7% because of the UHI effect. This study provides insights into the UHI in Beijing and recommendations to improve building design and decision-making while considering the urban microclimate.

Keyword: Urban heat island, Microclimate, Building design, Temporal and spatial characteristics, Beijing

1. Introduction

Many countries, especially developing countries, have experienced rapid urbanization over the last few decades. The proportion of the world's population in urban areas has increased from 30% in 1950 to 54% in 2014 and is projected to be up to 66% by 2050 [1]. Globally, China had the largest urban population in 2014, with 758 million urban dwellers, accounting for 20% of the world's total. The urbanization rate of China is predicted to reach approximately 70% by 2030 [2].

The rapid urbanization in major cities worldwide has created many issues, including the urban heat island (UHI) effect, a phenomenon that the urban area of a city is hotter than the rural area that surrounds it. Luke Howard was the first to recognize this effect and found that temperatures in London were 3.7 ℃ warmer than they were in the countryside at night [3]. Since then, this phenomenon has been reported in many other urban areas worldwide, such as the Greater Athens area [4], Nicosia [5], Vienna [6], and Mexico City [7]. In Asia, specifically, the UHI effect was found by many studies as well [8-16]. For example, examination of station records have indicated perceptible temperature increases in the urban area of Singapore [8]. The distribution maps of land surface temperatures on different times proved the significant UHI in Tokyo metropolitan area [9]. The cause of this phenomenon included the change of natural land surface and the high activities of production [10]. The UHI intensity in Korea was found more significant in inland cities than coastal cities [11]. In China, scholars have also put much effort into urban microclimate research. A study on the UHI in the city of Xiamen was carried out using remote sensing technology [12]. The results showed that development of an urban heat island in Xiamen was evident during the 11 years from 1989 to 2000, due to the expansion of the urban population. A study on the UHI in Chongqing, a city in Southern China, showed that the maximum UHI intensity occurred around midnight, and was as high as 2.5℃ [13].

Scholars took years to understand the characteristics of UHI in Beijing [14-19]. By comparing the surface air temperature data between one urban and one rural station between 1977 and 2000 in Beijing, it was found that the UHI intensity was strongest in winter and in the late nighttime or evening [14]. Yang et al. [15] analyzed the UHI in Beijing using monitored weather station data from 2007 to 2010.

Beijing's multiple ring road (RR) system of transportation was used in their study to divide the city into different areas. The weather sites inside the 6th RR were considered urban stations, with those inside the 4th RR central urban stations. They found that the largest UHI intensity generally took place inside the 4th RR whereas the areas near the northern and southern sections of the 6th RR experienced the weakest UHI phenomenon. Zhang [16] indicated that the temperature difference was approximately 4-6 ℃ between Beijing city and suburb area, and 8-10 ℃ between Beijing city and outer suburb area in 2001. Qiao et al. [17] reported that urban design based on urban form would be effective for regulating the thermal environment, due to the contributing influence of the encroachment of urban land on rural land on UHI effect.

The diurnal and seasonal features of UHIs have been investigated in many studies. It is widely accepted that the UHI intensity is greatest at night [20-22]. That is mainly because of the different cooling rates for the urban and rural areas at night and the large heat storage in the urban surfaces [23, 24]. There is no such consensus regarding the seasonal characteristics of UHIs. Basically, seasonal variation is related to the differences in the local weather conditions [25]. Chow et al. [20] reported that higher UHI intensity generally occurred during the southwest monsoon period from May to August in Singapore. Jongtanom et al. [25] found that the UHI effect was strongest during the dry season (November–April) and weakest during the rainy season (May–October) in Thailand. Zhang et al. [24] reported the strongest UHI intensity for Shanghai was found in autumn.

Many factors contribute to UHIs, of which the major ones were summarized by Oke et al. as follows [26]: decreased long-wave radiation loss, increased thermal storage in the building fabric, released anthropogenic heat, urban greenhouse effect, decreased effective albedo of the system due to multiple reflection, and reduction in evaporating surface in the city. In general, city buildings are regarded as a major contributing factor to UHIs. In addition, the dominant factors involved in the night time urban heat island energy budget at building level were analyzed by Schrijvers et al [27]. It was found that the long wave trapping effect is the main mechanism controlling the surface temperature.

There are two types of UHI: surface UHI, which refers to the difference in land surface temperature between the urban and rural areas, and atmospheric or near-surface UHI, which is defined as the difference in air temperature [28]. Moreover, atmospheric UHI can be distinguished further into that of the urban boundary layer (UBL) and that of the urban canopy layer (UCL) [29]. In the buildings field, the UCL-UHI is the most crucial and is related to people's lives because they live in the canopy layer.

The canopy air temperature directly affects outdoor thermal comfort and public health [30]. Therefore, in our study, we focused mainly on the characteristics of the UCL-UHI.

Phelan et al. [31] reviewed the literature to date and summarized the major direct and indirect impacts of UHIs. UHIs directly influence both daytime and nighttime temperature and indirectly increase air-conditioning loads, deteriorate air and water quality, reduce pavement lifetime, exacerbate heat waves, and so on. To mitigate the UHI effect, the simple ways are the use of reflective surfaces and planting of urban vegetation, which could save $10 billion in energy and equipment costs and eliminate 27 million metric tons of CO_2 emissions [32, 33].

The impact of UHIs on building energy use, to be specific, has been well documented across various climate conditions in the existing literature. In London, Kolokotroni et al. found that the rural reference building consumed 84% of the energy of a similar urban office during a typical hot week [34]. The annual urban cooling load was up to 25% higher than that of the rural area, and the annual heating load was reduced by 22% because of the London heat island effect [35]. In central Athens, Hassid et al. reported that the increase in cooling energy and peak demand due to a UHI was as much as 100% in 1997 and 1998 [36]. The study by Akasaka et al. confirmed that the cooling load had increased about 20% since 1900 whereas the heating load had decreased by 40% because of the heating island phenomenon in Tokyo [37]. Lowe [38] indicated that there is a net energy benefit due to the UHI in northern areas with cold climate in the US, whereas warmer areas use more energy because of the UHI. The effect of Modena's UHI on building energy consumption was also investigated [39]. Santamouris et al. [40] reviewed the existing studies concerning energy impact of UHI and found that in average the cooling load of typical urban buildings is 13% higher than rural buildings.

There is much evidence proving the significant energy impact of UHIs on buildings. However, only a few studies have paid attention to such impact in mainland China, though Li et al. found that Beijing's UHI accounted for almost 28.88% of that city's total air-conditioning consumption in 2005 [41]. In general, the UHI effect has not been fully considered in building design in China to date. For example, in Beijing, the capital of China, the available weather dataset in the current national design codes [42], [43] and the building simulation software comes from weather stations located in the urban area. Given there is a significant distinction of the climate conditions between the urban and rural areas [13], using the dataset from one station to represent all the regions of Beijing can cause a great deal of deviation in building design. Thus, the impact of the UHI on building thermal and energy performance may not be reflected effectively [44]. In addition, a limited number of studies have examined the long-term characteristics of a UHI in view of global climate change. According to the Intergovernmental Panel on Climate Change (IPCC) report, the globally averaged combined land and ocean temperature showed a warming of approximately 0.72 ℃ from 1951 to 2012 [45]. Therefore, the characteristics of a recent UHI can differ greatly from a decades-old UHI. Given that buildings can have a life cycle of more than 50 years, a full understanding of the long-term features of a UHI is essential for better building design, considering the urban microclimate. The goal of this study was to address these gaps in the present literature.

The temporal and spatial characteristics of the UHI in Beijing from 1961 to 2014 were investigated in this study. Furthermore, the impact of a UHI on building design, including design weather conditions, building energy consumption, and peak loads, were studied. The aim of this paper was to answer the following significant questions about the UHI in Beijing. (1) To what extent does the UHI influence the urban microclimate in Beijing? (2) How does UHI intensity change over the long term? (3) How large is the variation in weather condition, as caused by the UHI in different regions? (4) To what extent does the UHI influence building design and energy performance?

The rest of the paper is organized as follows. First, the source data and methodology are introduced in Section 2. Section 3 depicts and presents analyses of the UHI in Beijing. The temporal and spatial characteristics of the UHI, as well as the specific regional discrepancy, are analyzed further. In addition, the impact of the UHI on building design, including both the design weather conditions and energy performance, are discussed in Section 4. In the last section, conclusions are drawn based on the analysis results.

2. Method

2.1. Beijing weather stations and sources of weather data

Beijing is located in northern China and has a semi moist monsoon continental climate. As the important economic and political heart of the country, Beijing has a very dense population and high urbanization rate. The total population in 2014 was about 20 million and an average of 4.4% of the city's population migrated from its rural area to its urban area annually from 1990 to 2014 [1].

The weather data from 17 meteorological stations in Beijing, including seven urban stations and 10 rural stations, were used in this study. Among the area's weather stations, the Beijing station is traditionally used to represent the climate condition of all of Beijing for current design codes. The relative location of each weather station is shown in **Fig. 1**. The weather data were monitored and recorded by the Beijing Meteorology Service. The data period is from 1961 to 2014 for all the stations, except Haidian, Tanghekou, and Shijingshan, which had data records of 40 years, 41 years, and 38 years, respectively. The stations differed greatly in elevation, varying from 29.6 m (Shunyi) to 489.4 m (Yanqing), because the urban section of the city is located on a plain and is surrounded by mountains in the rural north and west areas. The Yanqing, Tanghekou, and Shangdianzi stations are situated in the mountains. To negate the impact of the different topographies of the stations, the air temperature observed at each station was corrected to the average elevation of the plain area based on the lapse rate. The lapse rate of temperature was recognized as 6 °C/km according to the International Civil Aviation Organization [46]. Detailed information and corrected temperature of each weather station are listed in **Table 1**.

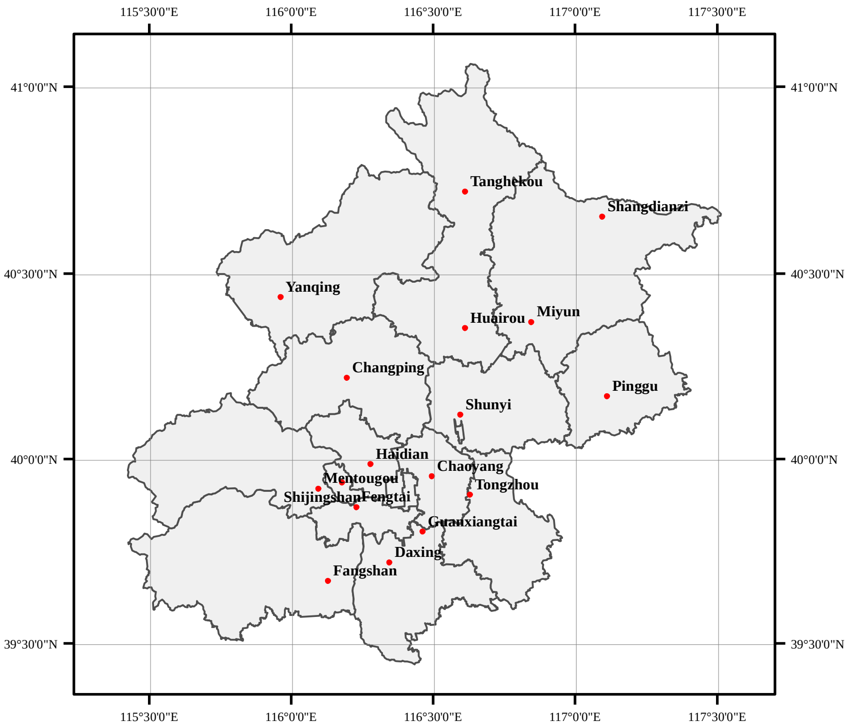

Fig. 1. Relative locations of the 17 weather stations in Beijing

Table 1. Detailed information about the 17 weather stations

Station Name	Shunyi	Haidian	Yanqing	Tanghekou	Miyun	Huairou	Shangdianzi	Pinggu	Tongzhou
Latitude	40°7’	39°59’	40°26’	40°43’	40°22’	40°21’	40°39’	40°10’	39°54’
Longitude	116°36’	116°17’	115°58’	116°37’	116°51’	116°37’	117°6’	117°7’	116°38’

Elevation (m)	29.6	46.9	489.4	333.7	73.4	75.6	286.5	32.1	44.5
Data Period	1961-2014	1975-2014	1961-2014	1974-2014	1961-2014	1961-2014	1961-2014	1961-2014	1961-2014
Total years	54	40	54	41	54	54	54	54	54
Adjusted Δt (℃)	-0.14	-0.04	2.62	1.68	0.12	0.14	1.40	-0.12	-0.05
Description	Rural	Urban	Rural	Rural	Rural	Rural	Rural	Rural	Urban
Station Name	Chaoyang	Changping	Mentougou	Beijing	Shijingshan	Fengtai	Daxing	Fangshan	
Latitude	39°57’	40°13’	39°55’	39°48’	39°56’	39°52’	39°43’	39°40’	
Longitude	116°30’	116°12’	116°6’	116°28’	116°11’	116°14’	116°21’	116°8’	
Elevation (m)	36.5	74.1	92.9	32.5	67.1	57	38.8	39.2	
Data Period	1961-2014	1961-2014	1961-2014	1961-2014	1977-2014	1961-2014	1961-2014	1961-2014	
Total years	54	54	54	54	38	54	54	54	
Adjusted Δt (℃)	-0.10	0.13	0.24	-0.12	0.09	0.02	-0.08	-0.08	
Description	Urban	Rural	Urban	Urban	Urban	Urban	Rural	Rural	

2.2. Index to measure the UHI intensity

To characterize the UHI intensity (UHII) quantitatively, an appropriate index should be determined first. Traditionally, UHII is defined as the difference in air temperature between the urban and rural stations [13], [44], [47], [48]. In some studies, UHII is quantified using the maximum difference between the urban temperature and the reference rural one [39], [49]. Although using these indices to measure UHII is easy to understand and simple to characterize, describing the duration of the UHI for a given period is difficult. As the temperature is a transient changeable climate condition, the accustomed UHII changes with every time step. These indices are useful to quantify the diurnal variation but not suitable for giving insight into the comprehensive discrepancy in UHII of different locations from a long-term perspective.

The California EPA developed a UHI index, defined in equation (1), to characterize and map UHIs in California in 2015 [50]. This index can capture both the severity (magnitude) and extent (duration) of the urban-rural temperature differential, and was therefore adopted in our study. In the definition equation, $T_{u,h}$ refers to the urban temperature at time-step h, whereas $T_{r,h}$ refers to the rural temperature at time-step h. H is the number of time-steps and k denotes the station index. The equation is used to calculate a cumulative UHII, in degree hours, over a designated period. In this study, the period refers to each calendar year from 1961 to 2014.

$$UHII = \sum_{h=1}^{H} \left[T_{u,k,h} - \min\left(T_{u,k,h}, T_{r,k,h} \right) \right] \quad (1)$$

The Beijing station, which is the traditional representative station in current design codes, was selected as the reference urban station. The other 16 stations were compared to the Beijing station and their UHIIs were calculated according to equation (1). The larger the UHII is, the more significant the difference from the urban area was at that station.

2.3. Spatial interpolation

For interpreting and visualizing the observed UHI in Beijing, it is important to know the spatial distribution of temperature at a specific time. Because the number of stations is limited, spatial interpolation is needed. Spatial interpolation is a feasible approach to predict the whole surface using discrete data points. There are numerous spatial interpolation methods, such as distance-weighting, Kriging, and spline interpolation methods [51]. In our study, a spline interpolation method was applied because spline interpolation methods are smoother, give more precisely located extrema, and draw a potential surface faster [52]. Moreover, it is the best method for representing the smoothly varying surfaces of phenomenon such as temperature [53] and the resulting smooth surface passes exactly through the input points. The detailed algorithm of the spline interpolation is introduced in the reference [54]. ArcGIS 10.4.1 software [55], developed by Environmental Systems Research Institute, was used to do the spatial analysis based on the weather data collected from the 17 observation stations. The default cell size is the shorter of the width or the height of the extent of the input point features, in the input spatial reference, divided by 250.

2.4. Reference building

A reference building was set up in DeST software [56] to evaluate the impact of the UHI in Beijing on building energy performance. DeST, which was developed by Tsinghua University in the early 1980s, is a common building simulation tool used in China. It is an appropriate tool for detailed analysis and evaluation of the building thermal process and energy performance. The reference building is a seven-story office building with a shape coefficient (the ratio of the building exterior surface area to the building volume) of 0.176. The U-values of the external walls, roofs, and windows are 0.5 W/m^{2}K, 0.4 W/m^{2}K, and 2.4 W/m^{2}K, respectively, according to the national design codes [42].

The internal heat gains are 10 m^2/occupant, 9 W/m^2 of lighting, and 15 W/m^2 of plug-load equipment. The infiltration rate is 0.5 h^{-1}. The air-conditioning system was assumed to be on with the set point temperature of 20 ℃ in winter and 26 ℃ in summer during working hours (07:00–18:00, Monday to Friday). The heating and cooling load of the reference building were calculated based on these settings.

3. Analysis of the UHI in Beijing

3.1. Spatial characteristics

To evaluate the UHI phenomenon in Beijing, spatial analysis was conducted first. Due to the different construction years of each weather station, the data record periods are distinct. The analysis period should be unified to avoid deviation brought by different climate conditions in different periods. In this study, the years from 1985 to 2014 were chosen because they are the most recent 30 years that are of reference value to the current situation. The air temperature for every time step of each weather station was corrected for by using each station's elevation according to Section 2.1. The mean temperatures of the four seasons during the most recent 30 years were calculated. Then, the spline interpolation was carried out to generate the temperature spatial distribution based on the mean temperature data points of the 17 stations. The spatial distribution made it possible to determine if a UHI existed and to what extent the urban and rural temperature disparity was because of the UHI in Beijing.

The results from the seasonal spatial distribution of temperature in Beijing are shown in **Fig. 2**. In general, the UHI phenomenon was found, but differed in magnitude, in all four seasons. In the winter months of December, January, and February (DJF), the UHI was the most significant across the four seasons. The temperature difference between the urban and rural areas reached a maximum of 6 ℃. In general, the center and southeast areas of Beijing experience the warmest winters. Regarding other seasons, the UHI in the summer months of June, July, and August (JJA) had the lowest differences. The discrepancy between the coldest and warmest areas was 4 ℃. The spatial variability in spring and autumn was larger than in summer but smaller than in winter. The temperature difference between the coldest and warmest areas was 5 ℃ in spring and autumn.

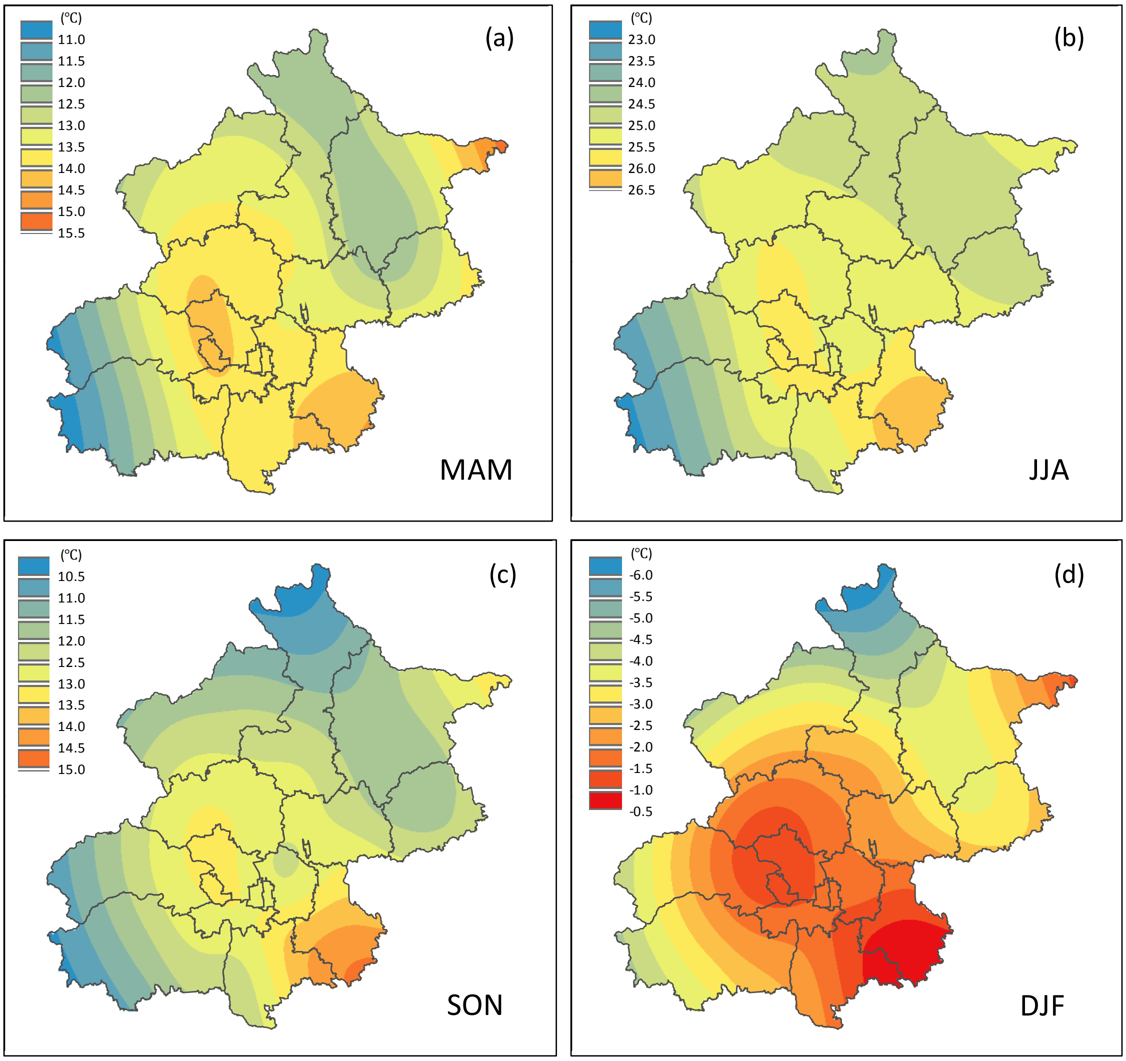

Fig. 2. Spatial distribution of average temperature in (a) March, April, and May (MAM); (b) June, July, and August (JJA); (c) September, October, and November (SON); and (d) December, January, and February (DJF) from 1985 to 2014

Notes: The lowest temperature point of each figure is the same color so that the darker shade of red of the high temperature area indicates a more significant temperature difference.

Fig. 3 shows the results of temperature distribution at the typical hours of midnight (00:00) and noontime (12:00), in summer and winter. The average temperatures at 00:00 and 12:00 in DJF and JJA from 1985 to 2014 were calculated. Consistent with the results in **Fig. 2**, the UHI in winter was more significant than it was in summer in Beijing. Concerning diurnal variation, the divergence was much larger during the daytime (12:00) than nighttime (00:00), regardless of season. The temperature difference due to the UHI was up to 8 ℃ during the winter nighttime, whereas it was only 2.5 ℃ during the summer daytime. This makes sense because the heat exchange between the urban and rural areas is obvious during the day because of the mixing of air, which is enhanced by the increasing temperature and convectively unstable air. During nighttime, the stable weather condition (e.g., calm wind) weakens the heat exchange, and the open space of the rural area usually promotes radiative cooling. Furthermore, more of the heat stored in building fabrics is released in the urban area than in the rural area during the night.

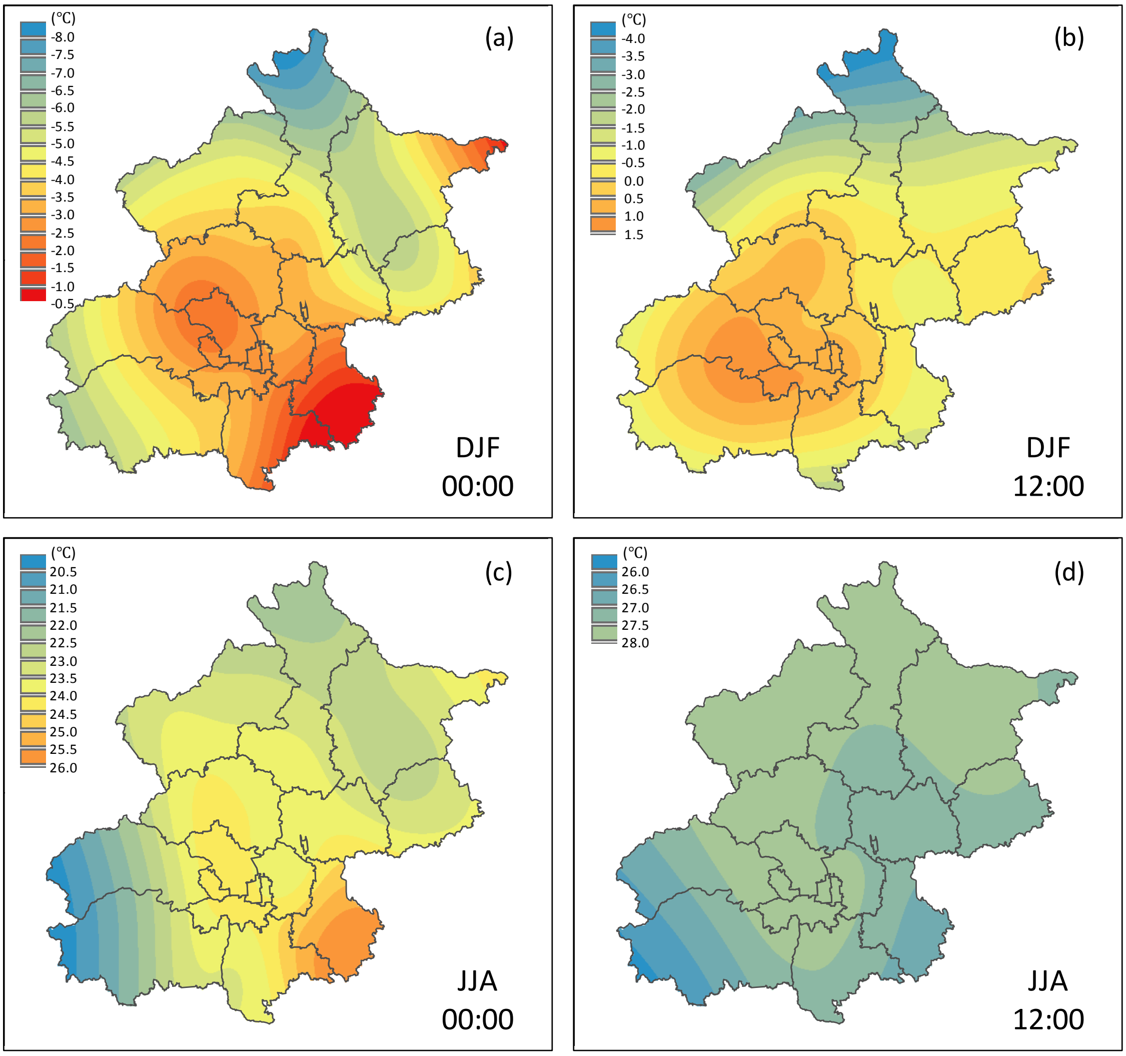

Fig. 3. Spatial distribution of average temperature in (a) DJF 00:00, (b) DJF 12:00, (c) JJA 00:00, and (d) JJA 12:00 from 1985 to 2014

3.2. Temporal characteristics

Studying UHII over a long period can help reveal the long-term temporal characteristics of the UHI phenomenon in Beijing. The UHII of each station compared to the reference urban station was calculated for each year. To show the general variation between the urban and rural stations, all 17 stations were categorized by type (urban or rural). The results are displayed in **Fig. 4**. In general, the

UHII was larger for the rural stations than for the urban stations, which is easy to understand. From a long-term perspective, the UHII varies significantly year by year. Three obvious abruptions in UHII were found during the period from 1961 to 2014. A sudden increase in UHII for most stations appeared around 1980 and again in 2003. On the other hand, a sudden decrease in UHII occurred around 1997. The literature shows that the UHI effect is somehow related to demographical and economic factors, such as built-up ratio and nonagricultural population density [57]. In Beijing, the abruption in UHII was potentially caused by macroeconomic factors. China experienced rapid development after the start of economic reform in 1978, which probably enhanced the UHII in 1980 because of the large-scale new construction and manufacturing, whereas the Asian financial crisis in 1997 may have resulted in the decrease in UHII in that year. The successful bid by Beijing for the Olympics in 2001 may have led to rapid development of the city, increasing the UHII for most stations in 2003.

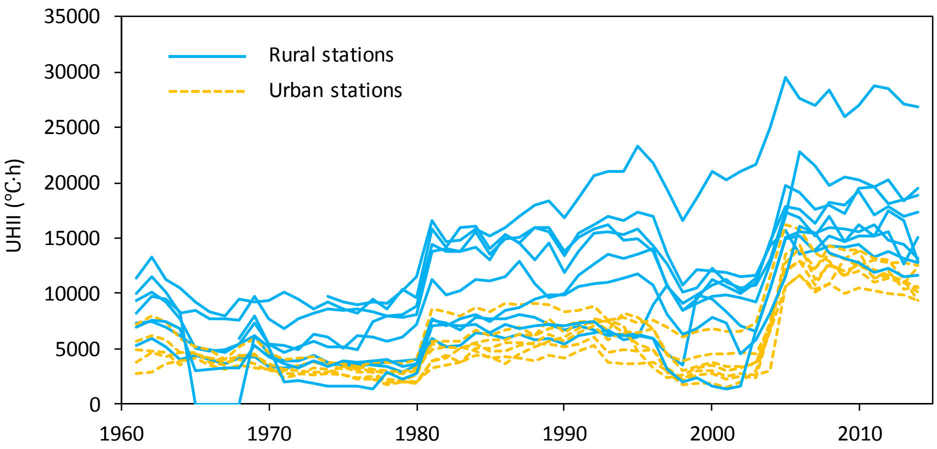

Fig. 4. Yearly change in UHII for urban and rural stations in Beijing from 1961 to 2014

To further analyze the potential impact of synoptic condition on the magnitude and development of the UHI, the Pearson correlation analysis was conducted in this study. The UHII in the various stations year-over-year was regarded as the independent variable and the annual average temperature and absolute humidity were the dependent variables. There are significant correlation between the UHII and the temperature and absolute humidity. The correlation coefficient between the UHII and the temperature was -0.351 with the significance of 0.000 and that between the UHII and the absolute humidity was -0.098 with the significance of 0.005. The bigger coefficient and smaller significance means the more significant the relationship is. Both correlation is negatively significant at the 0.01 level (significance <0.01) in this study. Namely, the cold and dry climatic condition would enlarge the

UHI effect in Beijing. The local climate influences the magnitude and development of the UHI together with the microeconomic factors.

3.3. Regional discrepancy

To compare the UHII of each station, a boxplot of annual UHII from 1985 to 2014 is shown in **Fig. 5**. In the figure, the 10 stations to the left are located in the rural area whereas the six to the right are in the urban area. The UHII of the urban area was generally from 3000 to 9000 degree hours during the most recent 30 years. Most rural stations had larger absolute values and relative changing ranges of UHII than the urban stations had. The most significant UHI effect was in Tanghekou, where the annual variation range between the Q1 and Q3 was approximately 15000 to 25000 degree hours, followed by Pinggu, Yanqing, and Miyun. The climate conditions of Shunyi and Changping were relatively similar to the urban stations regarding their annual variation in UHII from 1985 to 2014.

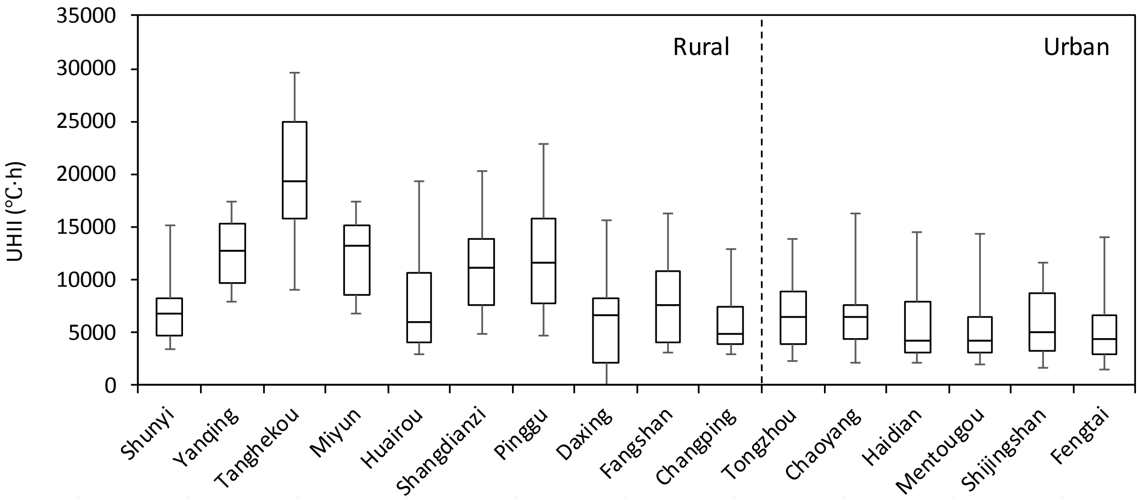

Fig. 5. Boxplot of annual UHII for different weather stations in Beijing from 1985 to 2014

3.4. Extreme events

Extreme air temperature is uncomfortable for humans and can even be lethal [47]. The indoor temperature can be 1.5℃-2.2℃ higher in a non-conditioned urban building than in the rural one due to the heat wave [59]. Thus, investigating the impact of a UHI on extreme events is necessary. Extreme events in this study refer to extreme hot days, when the daily average air temperature is higher than 30 ℃, and extreme cold days, when the daily average air temperature is lower than -10 ℃. It is noted that the temperature in this section was not corrected for by elevation in order to reveal the actual weather conditions.

The annual extreme hot and cold days for each station from 1985 to 2014 are shown in **Fig. 6** and **Fig. 7**, respectively. Regarding the extreme weather days in each year, two conclusions were made. First, the difference between the rural and urban areas in the number of extreme cold days was much more significant than it was in the number of extreme hot days in Beijing. The urban area had slightly more extreme days and nearly no extreme cold days, whereas cold days occurred more frequently in the rural area. Secondly, climate change in these years increased the frequency of extreme hot days drastically. Until 1996, the occurrence of extreme hot days was very rare, at close to zero each year. However, from 1997 on, extreme hot days appeared almost annually, with high peaks in 1999, 2000, and 2010 of more than on average 10 extreme hot days. The impact of climate change on extreme cold days was relatively less obvious.

	1985	1986	1987	1988	1989	1990	1991	1992	1993	1994	1995	1996	1997	1998	1999	2000	2001	2002	2003	2004	2005	2006	2007	2008	2009	2010	2011	2012	2013	2014
Shunyi	0	0	0	0	0	1	0	1	0	0	0	0	9	2	10	5	1	5	1	1	2	0	2	0	2	10	0	0	1	4
Yanqing	0	0	0	0	0	1	0	1	0	0	0	0	6	0	6	5	1	6	0	1	3	0	0	0	2	13	0	1	2	2
Tanghekou	0	0	0	0	0	0	0	1	0	0	0	0	6	0	7	2	0	2	0	0	2	0	0	0	0	6	0	0	1	2
Miyun	0	0	0	0	0	0	0	0	0	0	0	0	5	1	9	10	3	4	3	1	2	0	1	0	1	8	0	0	0	2
Huairou	0	0	0	0	0	1	0	1	0	0	1	0	4	0	7	3	1	5	1	1	1	0	0	0	1	6	0	0	0	2
Shangdianzi	0	0	0	0	0	1	0	1	0	0	0	0	9	0	11	15	0	5	0	1	2	0	1	0	1	6	0	0	1	2
Pinggu	0	0	0	0	0	1	0	0	0	0	0	0	9	1	15	9	1	8	1	1	4	0	1	0	0	4	0	0	0	4
Daxing	0	0	0	0	0	0	0	0	0	0	0	0	6	3	11	18	5	7	0	0	3	0	0	0	2	13	1	3	4	4
Fangshan	0	0	0	0	0	0	0	0	0	0	0	0	3	1	4	5	0	5	0	1	9	0	0	0	1	8	0	0	1	2
Changping	0	0	0	1	0	1	0	0	0	1	0	0	12	3	13	16	5	7	2	2	8	0	2	2	6	13	0	2	7	10
Tongzhou	0	0	0	0	0	0	0	0	0	1	1	0	8	4	16	19	6	8	3	2	7	1	3	2	6	13	2	3	7	12
Chaoyang	0	0	0	0	0	0	0	0	0	0	0	0	3	0	10	8	4	5	0	0	0	0	3	3	4	11	1	2	7	5
Haidian	0	0	1	1	0	0	0	1	0	0	0	0	10	3	15	15	7	8	3	1	6	0	2	3	5	12	0	0	1	3
Mentougou	0	1	0	0	0	0	0	1	0	0	0	0	9	2	12	14	4	7	2	1	8	1	1	0	4	12	0	1	2	12
Guanxiangtai	1	0	1	1	0	0	0	2	0	1	1	0	5	2	13	14	3	6	2	2	9	2	3	1	4	14	1	4	5	4
Shijingshan	0	1	1	0	0	1	0	2	0	1	0	0	11	2	12	16	4	6	2	1	8	0	2	0	5	13	0	2	6	8
Fengtai	0	0	1	0	0	0	0	1	0	2	0	0	9	3	15	20	6	10	3	2	11	0	2	0	4	14	0	1	5	4

Fig. 6. Annual extreme hot days for each station in Beijing from 1985 to 2014

	1985	1986	1987	1988	1989	1990	1991	1992	1993	1994	1995	1996	1997	1998	1999	2000	2001	2002	2003	2004	2005	2006	2007	2008	2009	2010	2011	2012	2013	2014
Shunyi	3	3	2	1	0	2	0	0	0	0	0	0	2	1	0	8	7	0	0	0	0	1	0	0	1	6	0	3	3	0
Yanqing	10	7	8	1	2	4	2	0	11	0	0	0	6	2	0	13	9	6	3	3	0	1	0	1	1	9	0	5	3	0
Tanghekou	15	7	7	3	2	7	5	0	10	5	1	2	10	4	5	16	8	8	7	7	6	7	0	10	6	20	13	20	16	1
Miyun	10	8	6	3	0	5	1	0	3	1	0	1	5	2	0	14	8	0	3	1	0	1	0	1	2	11	0	8	8	0
Huairou	3	2	2	0	0	2	0	0	0	0	0	0	4	3	0	8	8	4	2	2	0	1	0	0	2	13	0	6	4	0
Shangdianzi	8	3	3	2	0	2	2	0	3	3	0	0	6	3	2	9	7	0	3	2	0	1	0	3	3	10	1	10	8	0
Pinggu	5	4	6	2	0	8	1	0	0	0	0	0	5	2	0	7	7	1	2	1	0	2	0	1	2	9	0	6	2	0
Daxing	1	2	2	1	0	2	0	0	0	0	0	0	3	1	0	0	2	0	1	0	0	0	0	0	0	6	0	0	0	0
Fangshan	1	2	3	1	0	3	0	0	1	1	0	0	4	1	0	4	5	3	1	0	0	0	0	0	0	7	0	2	3	0
Changping	1	3	2	1	0	3	0	0	0	0	0	0	1	2	0	2	3	0	0	0	0	0	0	0	2	6	0	3	1	0
Tongzhou	2	2	3	1	0	3	0	0	0	0	0	0	0	1	0	0	3	0	0	0	0	1	0	0	0	5	0	1	1	0
Chaoyang	1	2	3	1	0	2	0	0	0	0	0	0	4	1	0	0	5	0	0	0	0	1	0	0	0	6	0	0	1	0
Haidian	2	2	2	0	0	1	0	0	0	0	0	0	0	1	0	0	2	0	0	0	0	0	0	0	0	4	0	0	2	0
Mentougou	1	0	1	1	0	2	0	0	0	0	0	0	1	1	0	1	2	0	0	0	0	0	0	0	1	5	0	3	1	0
Guanxiangtai	1	2	2	1	0	0	0	0	0	0	0	0	0	0	0	2	4	0	0	0	0	1	0	0	0	3	0	0	0	0
Shijingshan	1	2	1	1	0	2	0	0	0	0	0	0	1	1	0	0	3	0	0	0	0	0	0	0	0	3	0	0	0	0
Fengtai	1	1	1	1	0	2	0	0	0	0	0	0	3	1	0	1	1	0	0	0	0	0	0	0	0	4	0	0	1	0

Fig. 7. Annual extreme cold days for each station in Beijing from 1985 to 2014

The relationship between the 30-year average UHII and the number of extreme days is shown in **Fig. 8**. There was a significant positive correlation between the UHII and the occurrence of extreme cold events, as indicated by an R^2 of 0.93. That is, in areas where the UHI effect was stronger, the frequency of extreme cold days was much lower. A negative correlation was found between the UHII and extreme hot events. In summary, the UHI phenomenon increased the occurrence of extreme hot events but decreased the number of extreme cold days. It should be noted that the equation showed in the figure is a preliminary representation of the change trend of the number of extreme days accordance with different UHII. It cannot be used for predicting the occurrence of the extreme events, due to the limitation of the number of stations.

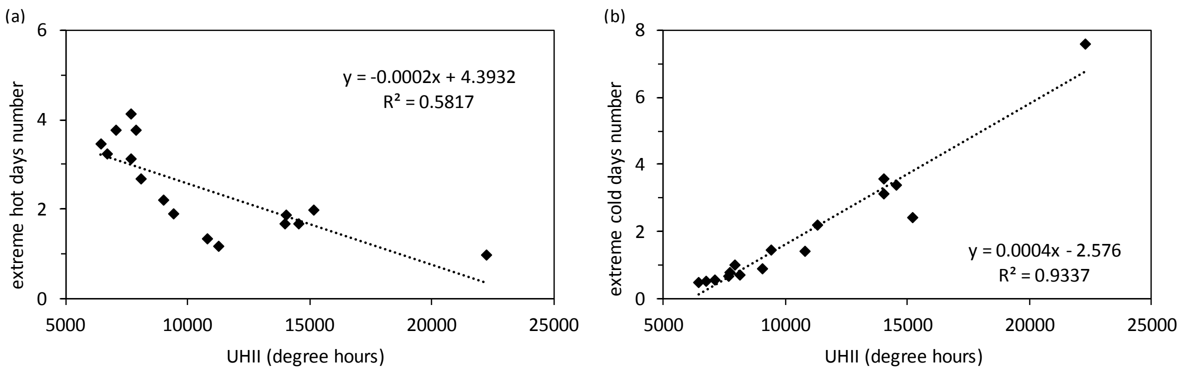

Fig. 8. Relationship between the annual average UHII and (a) the number of extreme hot days or (b) the number of extreme cold days for the 17 stations in Beijing (Each dot on the figure denotes a meteorological station.)

4. Impact of the UHI on building design and energy performance

To analyze the impact of the UHI on building design and energy performance, two aspects are discussed in this section: 1) the design weather conditions for building cooling and heating loads estimation and HVAC equipment sizing; 2) the simulated building annual thermal loads and peak loads for comparative study and building performance evaluation. The temperature mentioned in this section denotes the original recorded temperature, that is, the air temperature was not corrected according to elevation in order to reveal the actual building energy performance.

4.1. Design weather conditions

The major design weather conditions, compiled according to the national design code [43], for the different stations are listed in **Table 2**. The data from 1985 to 2014 were selected to generate the design conditions. Among all the stations, the Beijing station was generally the only representative station of the Beijing area. Nevertheless, the design parameters were distinguishable in the different regions, especially the rural and urban areas, because of the UHI phenomenon. Heating degree days based on 18 ℃ (HDD18) varied from 3715.8 ℃·d to 2807.2 ℃·d in the rural area and from 2724.3 ℃·d to 2826.0 ℃·d in the urban area. Regarding cooling degree days based on 26 ℃ (CDD26), the variation was from 6.6 ℃·d to 74.5 ℃·d in the rural area and from 61.3 ℃·d to 85.1 ℃·d in the urban area. The differences in HDD18 and CDD26 between the urban and rural areas were significant. The results of the design temperature for heating in winter and for cooling in summer were similar. The differences between the maximum and minimum of the heating design temperature in winter reached up to 5.8 ℃. The differences in summer design cooling temperature, although smaller than those in winter, were still up to 2.7 ℃.

Additionally, we can conclude that due to the UHI effect found in Beijing, the reference Beijing station was the hottest of all the stations, having the lowest HDD18 and highest CDD18. If we use the dataset from the Beijing station to estimate building loads regardless of region in Beijing, no doubt, there will be over predicted cooling loads and underestimated heating loads.

Table 2. Design conditions of the 17 stations in Beijing (1985–2014)

Type	Station	HDD18 (℃·d)	CDD26 (℃·d)	Heating design dry-bulb temperature in winter (℃)	Cooling design dry-bulb temperature in summer (℃)
Rural	Shunyi	2869.6	67.6	-7.6	34.1
	Yanqing	3645.9	6.6	-12.0	31.7
	Tanghekou	3715.8	10.6	-12.4	33.3
	Miyun	3214.1	42.9	-9.3	33.5
	Huairou	2985.9	46.9	-8.7	33.6
	Shangdianzi	3353.5	18.5	-10.7	32.7
	Pinggu	3070.5	52.5	-8.7	33.5
	Daxing	2811.1	70.5	-7.1	34.0
	Fangshan	2903.9	55.2	-7.8	33.6
	Changping	2807.2	74.5	-7.5	34.4
Urban	Tongzhou	2754.9	85.1	-7.2	34.1
	Chaoyang	2826.0	64.9	-7.0	34.0
	Haidian	2756.7	80.6	-6.8	34.4
	Mentougou	2812.0	61.3	-7.1	34.0
	Shijingshan	2757.4	77.8	-6.9	34.3
	Fengtai	2785.5	79.9	-7.0	34.3
Reference (Urban)	Beijing	2724.3	85.1	-6.6	34.1

Fig. 9 presents the changing trend in the design temperature during different periods. The Beijing and the Miyun stations were chose as the typical urban and rural stations, respectively. It is obvious that the design temperatures in both winter and summer have an increasing trend. The increasing trend

of the summer design temperature was almost the same in the rural and urban areas, with an increase of 0.4 ℃ every ten years. The urban microclimate resulted in an approximate 1 ℃ increase in the summer design temperature during different periods. The difference was more significant in the winter design temperature, with an increase of up to 2.8 ℃ from 1985 to 2014, which agrees with the results that the UHI phenomenon was more significant in winter. The changing trend of the winter design temperature for these two typical stations differed greatly. The winter design temperature increased 0.7 ℃ every 10 years in the urban area, whereas the increase was 0.5 ℃ in the rural area.

These results show that the design weather conditions, in general, vary annually due to climate change, intensifying the impact of the UHI on building design, especially when designing the heating system for winter in recent years. Sustained emphasis should be placed on the urban microclimate to improve the peak loads estimation for building design.

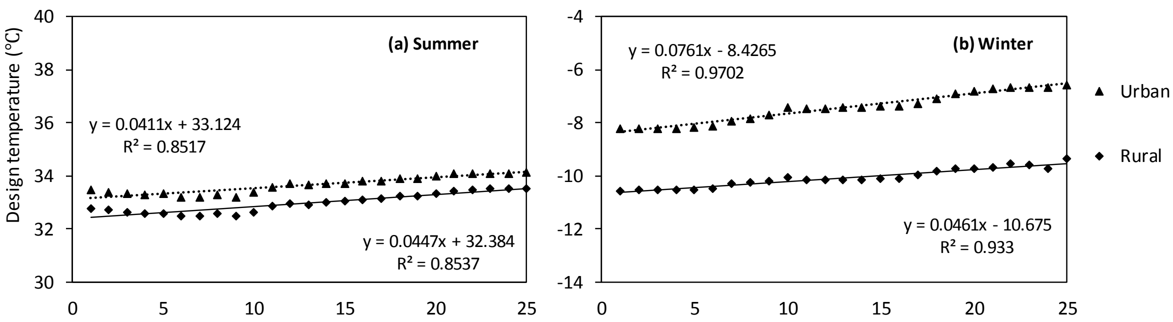

Fig. 9. Design temperature in (a) summer and (b) winter for the urban and rural stations in Beijing

Note: The *x*-axis of the figure refers to the different periods, for example, 1 denotes 1961–1990, 2 denotes 1962–1991, 3 denotes 1963–1992, and so on. The last point refers to the most recent 30 years, that is, 1985–2014.

4.2. Annual thermal loads and peak loads

The simulated heating and cooling loads are shown in **Fig. 10**. The weather data for the year 2000 for each station was selected as the weather data for the simulation, as the year 2000 was a relatively hot year in terms of extreme hot days, making it possible to investigate the impact of the UHI in a hot climate condition. The simulation results for different stations varied in both heating and cooling loads. The largest variations between the heating and cooling loads were 32.0 kWh/m^2 between Tanghekou and Beijing and 23.3 kWh/m^2 between Yanqing and Fengtai, respectively. The average heating load of the rural stations was 59.4 kWh/m^2 and 49.9 kWh/m^2 for the urban stations. The average cooling loads of the rural and urban stations were 56.2 kWh/m^2 and 62.6 kWh/m^2, respectively. This shows that the

UHI in Beijing led to an approximate 11% increase in cooling load and 16% decrease in heating load in the urban area compared to the rural area.

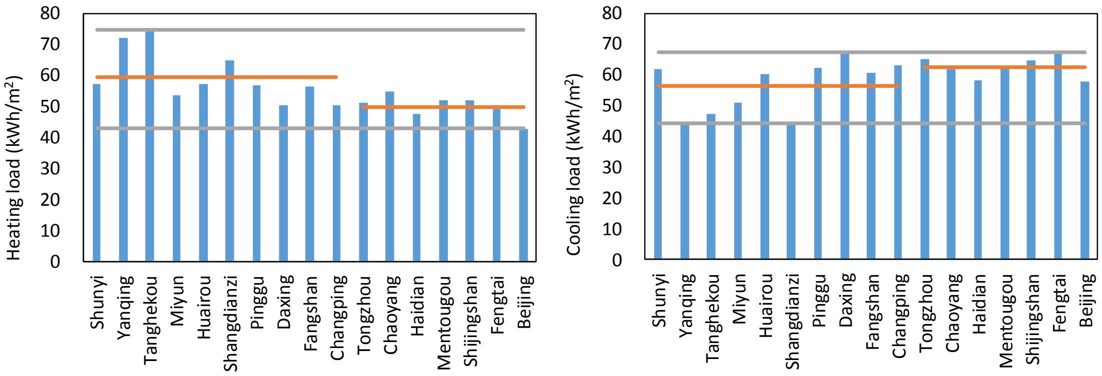

Fig. 10. Simulated loads of the reference office building in the year 2000 for different regions of Beijing

Note: The grey lines in the figure denote the maximum and minimum loads for all the stations.

Similar to the results of thermal loads, the urban microclimate demonstrates significant variations in peak loads, as shown in **Fig. 11**. The largest differences were 56.3 W/m^2 and 41.6 W/m^2 for the heating peak load and the cooling peak load, respectively, across all the regions. The variation was larger in the heating peak loads than it was in the cooling peak loads. The UHI effect resulted in a 9% decrease in the heating peak load as well as a 7% increase in the cooling peak load.

To estimate the electricity demand, we assume that the reference office building is equipped with the water-cooled centrifugal chillers with the COP (Coefficient of Performance) of 4.5. The peak electricity demand for heating and cooling are shown in **Fig. 12**. It was found that the winter peak electricity demand in urban area was in average 39.6 W/m^2, while that in rural area was about 43.3 W/m^2. The UHI in Beijing leads to approximately 8.5% decrease in peak electricity demand for heating. Conversely, the peak electricity demand in summer increased by 6.5% due to the UHI effect. The peak power demand for cooling was 27.7 W/m^2 and 26.0 W/m^2 in the urban and rural area, respectively.

In short, the building energy consumption and the peak load of various regions in Beijing can differ to a great extent. The UHI in Beijing had a more significant impact on building energy consumption than on the peak loads. In general, using the dataset from the Beijing station as the only weather input, not considering the differences in climate characteristics of the different regions, usually will underestimate the heating load and overestimate the cooling load, not only in the total consumption but also in the peak loads.

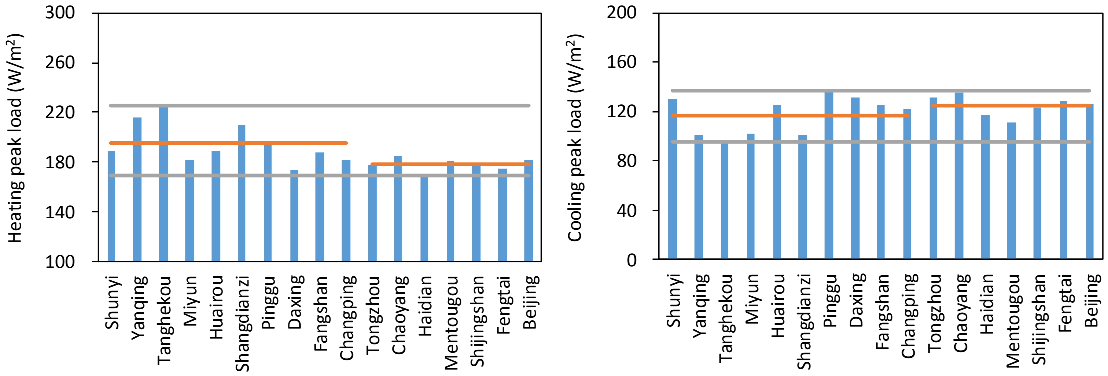

Fig. 11. Simulated peak loads of the reference office building in the year 2000 for different regions of Beijing

Note: The grey lines in the figure denote the maximum and minimum loads for all the stations.

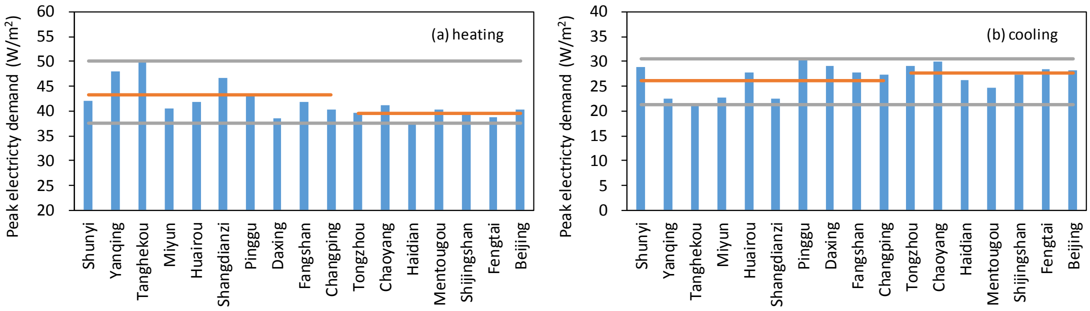

Fig. 12. Simulated peak electricity demand of the reference office building in the year 2000 for different regions of Beijing

4.3. Comparison with other cities

The energy impact of UHI in Beijing was compared to the results of other cities acquired from the literatures, as shown in **Table 3**. The comparison shows that the impact on the heating load in Beijing is larger than Modena, but smaller than London and Tokyo. Regarding the cooling load, the UHI in Beijing leads to a more significant increase than in Modena. The energy impact of UHI in Tokyo, London and Athens are larger than in Beijing. This results indicated that the influence of UHI on the building energy use is significant in the urbanized city all over the world, but the specific impact extent varies according to the local climatic conditions.

Table 3. The different energy impact of UHI between current study and literatures

No	City, Country	Data source	Impact on heating load	Impact on cooling load	Refs.
1	London, UK	Data from 24 locations in London for 2000	The annual heating load is reduced by 22%	The annual cooling load is increased by 25%	[35]

2	Athens, Greek	Data from 6 sites for 1997 and 1998	/	The cooling load is 67% and 29% higher than reference station in 1997 and 1998, respectively	[36]
3	Tokyo and Choshi, Japan	Data from 30 stations in a range of 100 km centering on Tokyo since 1900	The heating load of Choshi has decreased about 20%, and that of Tokyo has decreased about 40%	The cooling load of Tokyo and Choshi have both increased about 20%	[37]
4	Modena, Italy	Data from one station located in the city center and another in the surrounding area for 2011 and 2012	The heating load of suburban area are about 15% higher than that of urban area	The cooling load has increased by 10% than suburban area.	[39]
5	Beijing, China	Data from 17 stations in Beijing for 2000	The heating load in urban area is decreased by 16%	The cooling load increased by 11%	/

5. Conclusion

In this study, the weather data from ten rural stations and seven urban stations in Beijing since 1961 were investigated. Through deep and comprehensive analysis of the UHI effect in Beijing, this study increases the understanding of the temporal and spatial characteristics and the impacts on building design and energy performance of Beijing's UHI. The main findings of the study include:

1) The UHI effect in Beijing was significant. The UHI phenomenon was the most significant in winter, followed by autumn and spring. Summer was least influenced by the UHI effect. Meanwhile, the urban and rural temperature differences were much larger during the nighttime than during the daytime.
2) The UHII of most of the stations obviously changed around 1980, 1997, and 2003, partially due to microeconomic development.
3) The UHI led to an increase in the frequency of extreme heat events and a decrease in the occurrence of extreme cold events.
4) The building design and energy performance in different regions of Beijing can differ greatly, not only in the design weather parameters but also in the simulated building energy loads. Using only one reference station for the representative weather data may lead to a significant underestimate of heating design or overestimate of cooling design.

5) The heating load of urban area had decreased by 16% than that of rural area and the cooling load had increased by about 11% due to the UHI. Regarding the electricity demand, the UHI reduced the peak electricity demand from 43.3 W/m^2 to 39.6 W/m^2 in winter, and increased from 26.0 W/m^2 to 27.7 W/m^2 in summer compared to the rural area.

It is recommended that the UHI in Beijing be continuously monitored to remain cognizant of its trend. Design weather conditions and weather files for energy simulation should be from local weather stations, if available, to reduce the impact from using only the reference city weather station in urban areas. Understanding the temporal and spatial characteristics is the first step to developing effective strategies for mitigation of UHIs in cities.

Future research can expand the UHI impact simulation analysis for various building types with different energy systems and efficiency levels and can look at the whole building actual energy use (electricity and others). The dataset is also good for studies on heat waves and climate change in the Beijing region.

References

[1] United Nations, World Urbanization Prospects: The 2014 Revision. 2015, Department of Economic and Social Affairs, Population Division: New York.

[2] World Bank and the Development Research Center of the State Council, P.R.C., Urban China: Toward Efficient, Inclusive, and Sustainable Urbanization. 2014, World Bank: Washington, DC.

[3] Howard, L., The climate of London: deduced from meteorological observations made in the metropolis and at various places around it. 1833.

[4] Assimakopoulos M N, Mihalakakou G, Flocas H A, Simulating the thermal behaviour of a building during summer period in the urban environment. Renewable Energy, 2007. 32(11): 1805-1816.

[5] Theophilou M K, Serghides D, Estimating the characteristics of the Urban Heat Island Effect in Nicosia, Cyprus, using multiyear urban and rural climatic data and analysis. Energy and Buildings, 2015. 108: 137-144.

[6] Heiselberg, P.K., The scope and implications of the urban microclimate variance: a case study, in CLIMA 2016 - proceedings of the 12th REHVA World Congress. 2016.

[7] Jauregui, E., Heat island development in Mexico City. Atmospheric Environment, 1997. 31(22): 3821-3831.

[8] Tso, C.P., A survey of urban heat island studies in two tropical cities. Atmospheric Environment, 1996. 30(3): 507-519.

[9] Watanabe H, Yoda H, Ojima T, Urban environmental design of land use in Tokyo metropolitan area. Energy and Buildings, 1990. 15-16: 133-137.

[10] Ojima T., Changing Tokyo Metropolitan area and its heat island model. Energy and Buildings, 1990. 15-16: 191-203.

[11] Kim Y H, Baik J J. Daily maximum urban heat island intensity in large cities of Korea. Theoretical and Applied Climatology, 2004, 79(3-4): 151-164.

[12] Han-qiu X, Ben-qing C, Remote sensing of the urban heat island and its changes in Xiamen City of SE China. Journal of Environmental Sciences, 2004. 16(2): 276-281.

[13] Yao R, Luo Q, Luo Z, et al, An integrated study of urban microclimates in Chongqing, China: Historical weather data, transverse measurement and numerical simulation. Sustainable Cities and Society, 2015. 14: 187-199.

[14] Liu W, Ji C, Zhong J, et al, Temporal characteristics of the Beijing urban heat island. Theoretical and Applied Climatology, 2006. 87(1-4): 213-221.

[15] Yang P, Ren G, Liu W, Spatial and Temporal Characteristics of Beijing Urban Heat Island Intensity. Journal of Applied Meteorology and Climatology, 2013. 52(8): 1803-1816.

[16] Zhang J, Yao F. The characteristics of urban heat island variation in Beijing urban area and its impact factors. Urban Remote Sensing Event, 2009 Joint. IEEE, 2009: 1-6.

[17] Qiao Z, Tian G, Zhang L, et al. Influences of urban expansion on urban heat island in Beijing during 1989–2010. Advances in Meteorology, 2014, 2014.

[18] Zhou J, Li J, Yue J. Analysis of urban heat island (UHI) in the Beijing metropolitan area by time-series MODIS data. Geoscience and Remote Sensing Symposium (IGARSS), 2010 IEEE International. IEEE, 2010: 3327-3330.

[19] Wang J, Huang B, Fu D, et al. Response of urban heat island to future urban expansion over the Beijing–Tianjin–Hebei metropolitan area. Applied Geography, 2016, 70: 26-36.

[20] Chow W T L, Roth M, Temporal dynamics of the urban heat island of Singapore. International Journal of climatology, 2006. 26(15): 2243-2260.

[21] Magee N, Curtis J, Wendler G, The urban heat island effect at Fairbanks, Alaska. Theoretical and Applied Climatology, 1999. 64(1-2): 39-47.

[22] Vez J P M, Rodríguez A, Jiménez J I, A study of the urban heat island of Granada. International Journal of Climatology, 2000. 20: 899-911.

[23] Oke, T.R., The energetic basis of the urban heat island. Quarterly Journal of the Royal Meteorological Society, 1982. 108(455): 1-24.

[24] Zhang K, Wang R, Shen C, et al, Temporal and spatial characteristics of the urban heat island during rapid urbanization in Shanghai, China. Environmental monitoring and assessment, 2010. 169(1-4): 101-112.

[25] Jongtanom Y, Kositanont C, Baulert S, Temporal variations of urban heat island intensity in three major cities, Thailand. Modern Applied Science, 2011. 5(5): 105.

[26] Oke T R, Johnson G T, Steyn D G, et al, Simulation of surface urban heat islands under 'ideal'conditions at night part 2: diagnosis of causation. Boundary-Layer Meteorology, 1991. 56(4): 339-358.

[27] Schrijvers P J C, Jonker H J J, Kenjereš S, et al. Breakdown of the night time urban heat island energy budget. Building and environment, 2015, 83: 50-64.

[28] Van Hove L W A, Jacobs C M J, Heusinkveld B G, et al, Temporal and spatial variability of urban heat island and thermal comfort within the Rotterdam agglomeration. Building and Environment, 2015. 83: 91-103.

[29] Oke, T.R., The distinction between canopy and boundary-layer urban heat islands. Atmosphere, 1976. 14(4): 268-277.

[30] Xu Y, Liu Y, Monitoring the Near-surface Urban Heat Island in Beijing, China by Satellite Remote Sensing. Geographical Research, 2015. 53(1): 16-25.

[31] Phelan P E, Kaloush K, Miner M, et al, Urban Heat Island: Mechanisms, Implications, and Possible Remedies. Annual Review of Environment and Resources, 2015. 40(1): 285-307.

[32] Akbari H. Energy Saving Potentials and Air Quality Benefits of Urban Heat Island Mitigation. Lawrence Berkeley National Laboratory, 2005. Available at: http://escholarship.org/uc/item/4qs5f42s

[33] Rosenfeld A H, Akbari H, Bretz S, et al. Mitigation of urban heat islands: materials, utility programs, updates. Energy and buildings, 1995, 22(3): 255-265.

[34] Kolokotroni M, Giannitsaris I, Watkins R, The effect of the London urban heat island on building summer cooling demand and night ventilation strategies. Solar Energy, 2006. 80(4): 383-392.

[35] Kolokotroni M, Zhang Y, Watkins R, The London Heat Island and building cooling design. Solar Energy, 2007. 81(1): 102-110.

[36] Hassid S, Santamouris M, Papanikolaou N, et al, The effect of the Athens heat island on air conditioning load. Energy and Buildings, 2000. 32(2): 131-141.

[37] Akasaka H, Nimiya H, Soga K, Influence of heat island phenomenon on building heat load. Building Services Engineering Research and Technology, 2002. 23(4): 269-278.

[38] Lowe S A. An energy and mortality impact assessment of the urban heat island in the US. Environmental Impact Assessment Review, 2016, 56: 139-144.

[39] Magli S, Lodi C, Lombroso L, et al, Analysis of the urban heat island effects on building energy consumption. International Journal of Energy and Environmental Engineering, 2014. 6(1): 91-99.

[40] Santamouris M. On the energy impact of urban heat island and global warming on buildings. Energy and Buildings, 2014, 82: 100-113.

[41] Li C, Zhou J, Cao Y, et al., Interaction between urban microclimate and electric air-conditioning energy consumption during high temperature season. Applied Energy, 2014. 117: 149-156.

[42] Design Standard for Energy Efficiency of Public Buildings. 2015, China Architecture and Building Press: Beijing.

[43] Design code for heating ventilation and air conditioning of civil building. 2012, China Architecture and Building Press: Beijing.

[44] Chan, A.L.S., Developing a modified typical meteorological year weather file for Hong Kong taking into account the urban heat island effect. Building and Environment, 2011. 46(12): 2434-2441.

[45] Stocker, T.F., et al., Technical Summary, in Climate Change 2013: The Physical Science Basis. Contribution of Working Group I to the Fifth Assessment Report of the Intergovernmental Panel on Climate Change, T.F. Stocker, et al., Editors. 2013, Cambridge University Press: Cambridge, United Kingdom and New York, NY, USA. 33–115.

[46] International Civil Aviation Organization., Manual of the ICAO Standard Atmosphere: Extended to 80 Kilometres (262 500 Feet). 1994: International Civil Aviation Organization.

[47] Giridharan R, Ganesan S, Lau S S Y, Daytime urban heat island effect in high-rise and high-density residential developments in Hong Kong. Energy and Buildings, 2004. 36(6): 525-534.

[48] Kolokotsa D, Psomas A, Karapidakis E, Urban heat island in southern Europe: The case study of Hania, Crete. Solar Energy, 2009. 83(10): 1871-1883.

[49] Oke, T. City size and urban heat island, perspectives on wilderness: testing the theory of restorative environments. in Proceedings of the fourth world wilderness congress. 1987.

[50] Dean, W., Creating and Mapping an Urban Heat Island Index for California. 2015.

[51] Lam, N.S.-N., Spatial interpolation methods: a review. The American Cartographer, 1983. 10(2): 129-150.

[52] Perrin F, Pernier J, Bertnard O, et al, Mapping of scalp potentials by surface spline interpolation. Electroencephalography and clinical neurophysiology, 1987. 66(1): 75-81.

[53] Childs C. Interpolating surfaces in ArcGIS spatial analyst. ArcUser, July-September, 2004, 3235. Available at: http://webapps.fundp.ac.be/geotp/SIG/interpolating.pdf

[54] Mitáš L, Mitášová H. General variational approach to the interpolation problem. Computers & Mathematics with Applications, 1988, 16(12): 983-992.

[55] McCoy J, Johnston K, Environmental systems research institute, Using ArcGIS spatial analyst: GIS by ESRI. 2001: Environmental Systems Research Institute.

[56] Yan D, Xia J, Tang W, et al, DeST — An integrated building simulation toolkit Part I: Fundamentals. Building Simulation, 2008. 1(2): 95-110.

[57] Xiao R, Ouyang Z, Wang X, et al, Detecting and analyzing urban heat island patterns in Beijing, China. Research Center for Eco-Environmental Sciences. Chinese Academy of Sciences, Beijing, 2002. 100085.

[58] Michael Wehner, F.C., and Dáithí Stone, Extreme heat waves in a changing climate and their effect on human health and welfare. Oxford Research Encyclopedia of Natural Hazard Science, 2015.

[59] Riccardo P, Andrea Z, Maryam M, et al, The hygrothermal performance of residential buildings at urban and rural sites: sensible and latent energy loads and indoor environmental conditions. Energy and Building, 2016. http://dx.doi.org/10.1016/j.enbuild.2016.11.018